

Application of Auger and characteristic loss spectroscopies to the study of the electronic structure of Ti and TiO₂†

M. L. Knotek and J. E. Houston

Sandia Laboratories, Albuquerque, New Mexico 87115

(Received 27 December 1976)

Auger electron spectroscopy (AES) and core-level characteristic loss spectroscopy (CLS) have been employed as probes of the valence- and conduction-band density-of-states structures, respectively, in Ti and TiO₂. Both of the probes involve interactions with core levels which are highly localized so that the techniques are sensitive to local atomic environment as well as being surface sensitive. All of the data are treated using background subtraction and deconvolution procedures to remove the distorting effects of extrinsic losses suffered by the analyzed electron in its interaction with the solid. The AES results for the $L_{23}M_{23}M_{45}$ structure are directly compared with soft-x-ray emission (SXE) $L_{23}M_{45}$ spectra and a good overall agreement in line shape is obtained. The TiO₂ surface as analyzed has a valence structure indicating some surface reduction. The Auger results have a relative L_3 - L_2 weighting similar to the very high self-absorption case of SXE. The Ti L_{23} CLS spectra for both Ti and TiO₂ show good agreement to the equivalent Ti L_{23} soft-x-ray absorption (SXA) spectra in the raw state before the effects of extrinsic losses have been removed, which suggests that such processes are also present in SXA. In the case of Ti, comparison of the structures obtained from AES and SXA are compared to the band-structure calculations of Jepsen and show reasonable agreement although these spectroscopies broaden the structure considerably.

INTRODUCTION

In recent years there has been increasing interest directed toward the photoelectrolysis of water on semiconductor electrodes. It has been demonstrated that under suitable bias conditions, TiO₂ photoelectrolyzes water with quantum efficiencies near 100% for radiation above the band gap.¹⁻³ The properties of TiO₂ as a photocatalytic electrode in electrochemical cells have been rather extensively studied.⁴ One disadvantage of such studies is that the processes at the electrolyte-electrode interface are so complex that it is virtually impossible to isolate those directly involving the critical surface chemistry. It is in this area where modern surface techniques offer unique advantages. The studies reported here are part of a comprehensive examination of the surface photocatalytic properties of TiO₂ and deal specifically with the electronic characterization.

There has been some surface work on photolysis-related properties of TiO₂ semiconductor electrodes. Henrich *et al.* have used ultraviolet photoelectron spectroscopy (UPS) and near-elastic characteristic loss spectra to demonstrate the presence of Ti³⁺ defects which appear to play a crucial role in the catalytic activity of the surface.⁵ Naccache *et al.*,⁶ used paramagnetic-resonance techniques to study the adsorption of oxygen at such Ti³⁺ sites and Morin and Wolfram⁷ ascribe the catalytic properties of the d -band perovskites to the presence of this type of surface state. Boonstra and Mutsaers⁸ conclude that the nature of hydroxyl groups chemisorbed at these sites is

crucial to the mechanism of photolysis.

One of the key aspects pertinent to catalytic behavior is that of the detailed surface electronic properties. Several probes of these properties have been used over the years and several others are developing rapidly for such applications.⁹ Two of the most prominent are x-ray and uv photoelectron spectroscopies, which view surface chemistry in terms of the distribution of filled electronic states. Other techniques used for similar purposes include soft-x-ray emission spectroscopy (SXE) and Auger electron spectroscopy (AES). Techniques are also available for probing the distribution of empty electronic states and these include spectroscopies such as soft-x-ray absorption (SXA), core-level characteristic loss (CLS), soft-x-ray appearance potential (SXAPS), and bremsstrahlung isochromats. Of these various techniques, several involve the excitation or de-excitation of a deep core level (i.e., SXE, AES, SXA, SXAPS, and CLS) and these offer distinct advantages. These probes view valence- and conduction-band states in terms of transitions to a spatially localized core state and thus yield information about the electronic properties in the neighborhood of each particular surface atomic species. The SXE and AES techniques involve a spectral analysis of characteristic decay products (x rays in the former and electrons in the latter) resulting from transitions from the filled states (in our case, valence levels) to the core hole, and thus reflect the filled density of states. The SXA, SXAPS, and CLS techniques, on the other hand, involve excitation transitions from core states to

empty or conduction-band states and thus reflect their density distribution. In addition, AES and CLS have the advantage that they are accomplished using the same experimental apparatus and one which is common to almost all surface physics laboratories.

Unfortunately, such applications of AES and CLS are not widely found in the literature and as yet these probes are not well characterized with respect to their ability to determine surface electronic properties. A comparison with the better characterized techniques (SXA, SXE, UPS, etc.) is needed as well as comparisons to theoretical calculations. The major points to be investigated are the magnitude of many-body effects and oscillator strength variations (i.e., selection rules or matrix-element effects) on the spectroscopic results. No comparisons of this sort are known to exist for CLS, but several recent studies involving AES have shown encouraging results. For example, it has been shown that the Al,¹⁰ and Si,¹¹ *L*_{2,3} *V**V* structures can be characterized in terms of the calculated bulk band structure, without invoking many-body corrections, by noting that matrix-element effects cause states of *p*-like symmetry to be strongly emphasized. Solomon and Baun¹² have analyzed the Auger spectra of Ti and TiO₂ and have found that if the *LMV* line is decomposed into components, in a manner similar to Fischer's¹³ decomposition of the Ti and TiO_x SXE data, there is a reasonable agreement in the number of components present in the AES and SXE structures as well as their relative strengths. However, without proper data reduction, such as discussed in this paper, the significance of similarities or differences between the two bodies of data is uncertain. In the present paper, the results of AES and CLS applied to titanium and titanium oxide are reported and directly compared with the results of SXE, SXA, and theoretical calculations (for the case of Ti metal).

Although the surface-sensitive techniques are powerful because the strong electron-electron interaction in solids causes short inelastic mean free paths, such strong interactions cause two effects which must be considered if one is going to make meaningful comparisons. Straggling losses of the incident high-energy electron beam (1–5 keV) give rise to a secondary-electron background upon which the characteristic Auger features are superimposed. Similar losses suffered by the Auger electrons themselves produce a tail on the low-energy side of the peak which can distort the true shape of the peak. We correct for the background by using a method described by Sickafus¹⁴ and handle the distorting effect of loss processes suffered by the escaping Auger electrons by a de-

convolution procedure. This procedure involves deconvoluting, from the Auger feature, the near elastic structure found for electrons backscattered from the surface with incident energy equal to that of the Auger feature. The application of such techniques for this purpose has been described.¹⁵

The Auger structures for Ti and various Ti compounds have been published in their usual differential form by several authors.¹⁶ The major features are the result of *L*_{2,3} *M*₄₅ *M*₄₅ (i.e., *L**V**V*, where *V* is for valence), *L*_{2,3} *M*₂₃ *M*₄₅ (*LMV*), and *L*_{2,3} *M*₂₃ *M*₂₃ transitions. The *L*_{2,3} levels are spin-orbit split by 6 eV so that each line is a superposition of two components separated by 6 eV. The *L*₂ lines are expected to be weaker by at least a factor of 2 than those of the *L*₃. When seeking valence density-of-states information, it is logical to analyze the *LMV* line since the sharpness of the core levels make that structure, in the simplest picture, directly reflect the valence-band density of states. On the other hand, the *L**V**V* features should reflect the self-fold of the valence-band density of states to the first approximation. Herein we compare the *LMV* structure to *L*_{2,3} SXE spectra. For the case of CLS, we analyze the *L*_{2,3} loss edge, which should reflect the conduction-band density of states and compare this to the equivalent *L*_{2,3} SXA excitation edge.

The results of our comparison show an excellent overall agreement, the AES spectra being somewhat broader than the equivalent SXE and calculated structures. The weighting of the band structures with respect to valence-orbital symmetry appears to be similar to that found in SXE, although the intensity of the *L*₂ contributions is found to be weaker than expected. The CLS-SXA comparisons are quite good, but agree more closely in the raw form (before structures due to straggling losses have been removed) than in the reduced form, which may indicate that the x-ray absorption process is considerably more complicated than has generally been assumed.

EXPERIMENTAL

The AES and CLS data were taken on a tandem, retarding-grid cylindrical mirror analyzer described previously by Gerlach and Tipping.¹⁷ This analyzer has the advantage of constant resolution over the complete range of energies analyzed. The data are taken in the *dN/dE* mode with the differentiation being accomplished by the potential modulation technique.¹⁸ By choosing the particular mode of potential modulation, i.e., varying the incident beam energy and energy window together or simply the energy window, it is possible to sample either strictly Auger electrons, which have a

fixed energy relative to the solid, or strictly electrons which have suffered some characteristic loss (CLS) and have an energy which is fixed relative to the primary beam energy.¹⁹ This makes it possible to set the analyzed loss electron in the same energy range as Auger electrons without the complication of overlapping spectra.

All of the data were taken with a coaxial electron gun which had a focused beam roughly 0.5 mm in diameter. Beam currents of the order of 20 μA were used and the resolution of the instrument was set at ~ 1.5 eV for the measurements reported here. The data were taken in a vacuum system with a base pressure $< 1 \times 10^{-10}$ Torr which rose to $\sim 2 \times 10^{-10}$ Torr during analysis.

Data averaging was employed using a Nicolet Model 1074 signal averaging computer. After averaging, the data were transferred in digital form onto magnetic tape (using a Texas Instruments Model ASR 733 data terminal) and was subsequently transferred to a central, time-sharing computing facility where additional reduction was accomplished. Typical data runs in the case of Auger structures required 10–20 min while the CLS data required ~ 1 h of averaging.

To reduce the data, we adopt a procedure described earlier¹⁵ in which it is assumed that the result of losses suffered by the Auger electrons in leaving the solid can be adequately approximated by the near-elastic backscatter spectrum resulting from bombarding the surface with electrons with an energy nearly equal to that of the Auger feature to be analyzed. Including the elastic peak in this spectrum permits one to also correct for the resolution of the instrument. It is then assumed that a measured Auger feature consists of a "true" line shape convoluted with the loss function. Retrieving this true shape amounts to reversing the process or deconvoluting the backscatter structure from the measured Auger line shape.

The Ti samples were prepared by evaporation onto a Pt-foil substrate which was cleaned by resistive heating up to temperatures of 1200 °C. The Ti surface is so reactive and the AES-CLS spectra so sensitive to changes in band structure, that it was necessary to evaporate a new film of Ti at intervals as short as 10 min even at our working pressures. A high-temperature cleaning of the Pt ($T > 1100$ °C) preceded each sublimation of Ti and was adequate for removing all material including the previously deposited Ti from the substrate. The Pt ribbon was initially cleaned and heated to ~ 1100 °C in O_2 to remove carbon contamination.

The TiO_2 samples were single crystals of both *a*-axis and *c*-axis orientation which had been cut, polished, and etched by conventional techniques. The *c*-axis sample had been reduced ($\sim 10^{19}/\text{cm}^3$

bulk oxygen vacancies) in a hydrogen furnace to enhance the conductivity. There were no noticeable differences in the electron spectroscopic results between the *a* and *c* axis or between pure and bulk-reduced samples. Ion etching was necessary to remove surface contaminants such as carbon and subsequent exposure to oxygen was used to compensate for the reducing effect of the ion beam.⁵

RESULTS

The analysis process is illustrated in Fig. 1 for the L_{VV} structure of Ti. The Van Cittert scheme, which is an iterative, self-consistent numerical technique, is used to accomplish the deconvolution.²⁰ Figure 1(b) shows the Ti L_{VV} feature in its raw $N(E)$ state after integrating the background-corrected dN/dE spectrum. Figure 1(a) shows the backscatter structure at a near coincident energy, and Fig. 1(c) gives the result of the deconvolution procedure. In the simplest model, this resulting structure is made up of the self-fold of the valence-band density of states projected onto the L_2 and L_3 Ti core levels which are spin-orbit split by 6 eV.

Figure 2 illustrates the AES-SXE comparison. Shown in Fig. 2(a) is the comparison of the Ti LMV transition (after background subtraction, integration and deconvolution) and the $L_{2,3}$ SXE data of Fischer and Baun.²¹ The SXE data corresponds

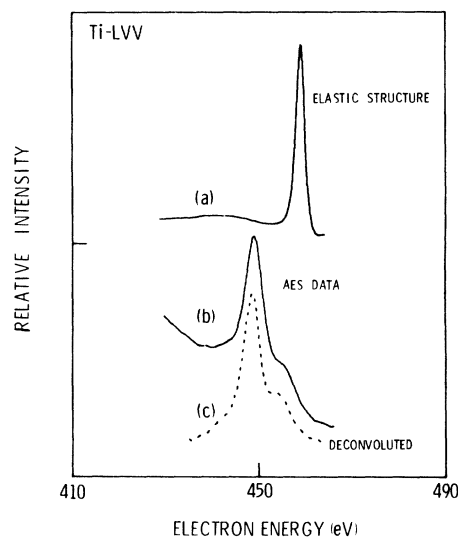


FIG. 1. Demonstration of the deconvolution procedure on the $L_{23}M_{45}M_{45}$ (L_{VV}) Auger structure for Ti. (a) is the elastic structure at a near coincident energy, (b) is the raw AES data after a background subtraction and integration, and (c) is the Auger structure after deconvolution. The resulting structure represents the self-fold of the valence-band density of states projected on the spin-orbit split L_3 and L_2 core levels.

to the high self-absorption case. The AES and SXE structures agree quite well in general shape with the SXE data, in this case, being somewhat sharper. The Auger peak appears to be close to its intrinsic width since there is little effect of instrument resolution on the peak width for resolution better than 1.5 eV. The low-energy shoulder on the Auger peak is due to a very low level of contamination (O, Cl, S). Figure 2(b) shows the Ti $L_{23}MV$ structure of a TiO_2 surface. The surface is reduced below stoichiometric TiO_2 and the comparison in Fig. 2(b) is to Fischer's Ti_4O_7 SXE results rather than those from TiO_2 due to their marked similarity. Higher oxidation states of the surface could be obtained by e -beam heating in O_2 . The agreement is quite good, both as to the relative shapes and sizes of the two major peaks in the structure (the low-energy feature is of $O2p$ origin while the high-energy peak is due to that of Ti $3d$), as well as the splitting of the two peaks. Note that the L_2MV transition in both cases shows comparison to the extremely high self-absorption case of SXE,²¹ i.e., the ratio of the L_3 to L_2 peak strength is $\gg 2$.

In Fig. 3 we compare the CLS and SXA data. The primary beam energy was 700 eV and the energy of the feature was ~ 240 eV. Figure 3(a) shows the Ti $L_{2,3}$ electron absorption edge which has been background-corrected and integrated, but not deconvoluted so that the features due to extrinsic losses are still present. This is compared to Fischer's Ti L_{23} x-ray absorption edge.²¹ In the classic picture of x-ray absorption we would expect that the detailed line shape should compare more

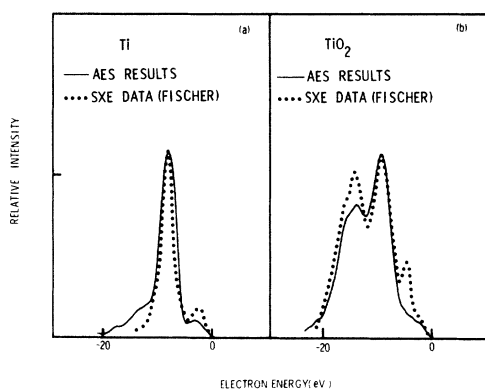


FIG. 2. Comparison of the $L_{23}M_{23}M_{45}$ (LMV) Auger structure after background subtraction and loss deconvolution (solid lines) and the $L_{23}M_{45}$ (LV) soft-x-ray emission data of Fischer (dotted lines) for (a) Ti and (b) TiO_2 . The SXE data plotted in (b) is for Ti_4O_7 . The Auger structures have a weaker L_2 contribution (the higher energy peak) than do the SXE structures. The various structures have been brought into coincidence in absolute energy for comparison purposes.

favorably to the deconvoluted CLS structure since SXA is generally thought to directly reflect the distribution of empty states without the loss processes normally encountered when electrons are involved. However, as can be seen, the raw CLS and SXA results are virtually identical. As expected, the deconvoluted CLS results, shown in Fig. 3(b), are sharper in character and the high-energy loss tail has been greatly reduced. In Figs. 3(c) and 3(d) are the equivalent comparisons of the TiO_2 CLS and the Ti_4O_7 SXA data and the deconvoluted TiO_2 CLS structure, respectively. Once again, there is a strong similarity between the raw CLS data and the SXA spectrum. It should be noted that when the oxygen K CLS edge was attempted on TiO_2 , the signal was immeasurably small. This effect was also seen in other transition-metal oxides in soft-x-ray appearance potential data.²²

We would expect that in the case of Ti the comparison of the properly reduced data with band-structure calculations should not yield unreasonable results. Figure 4 shows a comparison of the Ti L_3MV Auger line and the Ti L_3 characteristic loss results with the band-structure calculation of

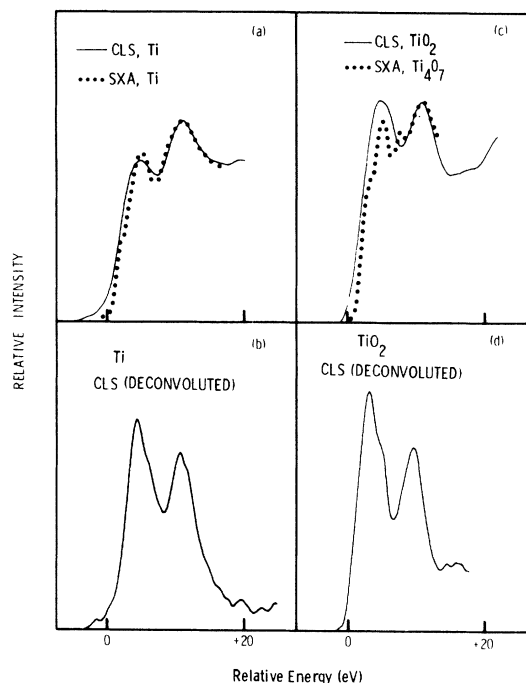


FIG. 3. Comparison of the L_{23} characteristic loss edge after background subtraction and integration (solid lines) to the equivalent L_{23} soft-x-ray absorption edge data of Fischer (dotted lines) for (a) Ti and (c) TiO_2 and Ti_4O_7 and after deconvolution for (b) Ti and (d) TiO_2 . Note the strong similarity between raw CLS data and SXA data. The structures were arbitrarily matched in absolute energy.

Jepsen.²³ We refer to the distribution of occupied states below the Fermi energy as the valence band and the empty-states distribution above the Fermi energy as the conduction band. The Auger process smears out the details considerably so that the d band splitting in the valence band is not evident in the AES line, but there appears to be a vestige of the two peaks in the conduction-band structure.

DISCUSSION

One of the fundamental questions to be answered by a direct comparison of AES and CLS data to the x-ray counterparts, SXE and SXA, is the sensitivity of oscillator strengths to orbital symmetry. X-ray emission and absorption is characterized by well defined, simple dipole selection rules $\Delta j = \pm 1$. Thus SXE and SXA data involving a K core hole will emphasize the p -like character of valence or conduction bands and an L core hole emphasizes s and d character. This is clearly demonstrated in Fischer's treatment of Ti and TiO.²⁴ The selection rules for the Auger transitions are somewhat more complex²⁵ and in general would not be expected to show strong similarities with SXE data. In our particular case, however, the results indicate a strong overall similarity. A similar situation has been reported for the $L_{23}VV$ transitions for Al,¹⁰ and Si,¹¹ where the Auger matrix elements favored transitions involving valence levels of p -like symmetry. Thus good agreement was obtained between AES and SXE for

L -shell holes. With respect to relative intensities of the L_3 and L_2 structures, however, it is quite apparent from our results that the Auger process results in an L_3 - L_2 ratio significantly greater than 2 (2 being the relative populations of the two levels). SXE in the case of minimum self-absorption shows an L_3 - L_2 ratio very close to 2. It is not clear at this point what the source of the effect is, but a similar ratio is apparent in AES results throughout the $3d$ series²⁶ rapidly returning to a value near 2 for Zn. A Coster-Krönig transition which would depopulate the excited L_2 levels could lead to such an effect but we would expect the depopulation to be apparent in the SXE spectra as well.

SXA has the same optic selection rules as SXE and, due to the strong Ti d character of the conduction band for both Ti and Ti compounds, we expect that the SXA L_{23} edge data should directly reflect the conduction-band density of states. Ludeke and Koma²⁷ have reported optic-like selection-rule effects in CLS core-level-to-surface-state spectra for primary energies $E_p \geq 100$ eV; E_p in the present instance is ~ 700 eV. Freeouf²⁸ on the other hand, finds that the apparent selection-rule effects of Ludeke and Koma can be easily explained assuming only a simple symmetry for the surface states together with exchange effects. This is, however, somewhat of a moot point in our case due to the dominance of states of d -like symmetry in the conduction band of both Ti and TiO₂. In the case of TiO₂, we can view the conduction-band states both from the viewpoint of Ti or O core levels. Since these core levels are quite localized spatially, the transition rates are sensitive to the local electronic properties. The fact that we see strong and weak structures for CLS lines involving Ti and O core levels, respectively, is taken as an example of the local nature of this probe. In the vicinity of the Ti sites, the local density of conduction-band states is dominated by the sharp d band which is highly localized on these sites. At the oxygen sites, however, one finds only states with s and p symmetries. Of course, the fact that the core-level states for Ti and O are of differing symmetries could give rise to the drastically reduced O K -level CLS result reported here. However, this strong a selection rule is not to be expected for electron excitation.

From the degree of overall agreement, it appears that many-body effects do not play a dominant role in the transitions encountered in the present work. However, there are several features of our results which could be ascribed to such effects. When core-levels are used to view valence- and conduction-band features, the results will be broadened by the core-level lifetime,

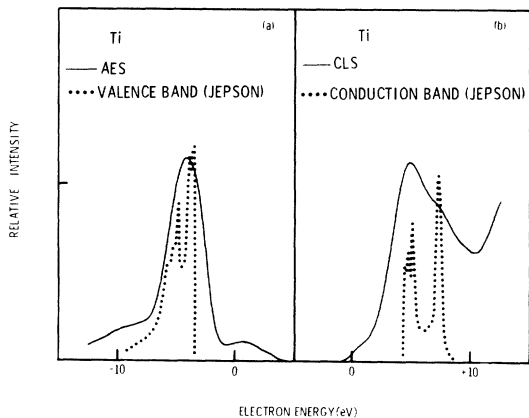


FIG. 4. Comparison of the (a) $L_3M_{23}M_{45}$ (LMV) AES line and the (b) L_3 characteristic loss edge structure for Ti to the valence- and conduction-band structures, respectively (dotted lines), calculated by Jepsen (Ref. 23). The Fermi level in both cases corresponds to the point where the dotted curves abruptly go to zero. The zeroes on the voltage axis simply show the scale and have no meaning with respect to the Fermi energy.

which, in our case, is predicted to be only ~ 0.25 eV.²⁹ In addition, the broadening due to the instability of the final two-hole configuration must be included. This state decays rapidly with the holes moving toward the Fermi level. The effects of hole-hole repulsion must contribute strongly to this instability. This phenomenon has not been investigated, but it seems clear that the additional broadening seen in the AES results compared to SXE could be due to such an effect.

The close agreement between uncorrected CLS and SXA results indicate that interactions with the solid by the excited core-electron play an important intrinsic role in the detailed absorption structure. Similar long-range interactions of the excited electron with the solid lattice are the origin of detail seen in extended x-ray absorption fine structure. This technique is finding increasing application as a probe of the radial distribution functions in solids. It is clear from our results, that these processes must be adequately accounted for if any meaningful comparison of SXA spectra with theory are to be made. The necessity of this kind of correction is also clearly illustrated by our AES results, where the distorting effects of loss processes on the line shapes is even more dramatic.

CONCLUSIONS

It is becoming quite well established that in addition to having the capability of accurately determining surface elemental composition, core-level electron spectroscopic techniques such as AES and CLS are unique and useful probes of surface electronic properties. Valence-band photoelectron and soft-x-ray photoemission spectroscopies have long been known for their sensitivity to the energy distribution of valence-band states, but in the former, this information is in the form of a spatial average and in the latter, surface sensitivity requires near-threshold excitation which results in an exceedingly difficult experiment. Although it is clear that the relationship between the spectral line shapes and the distribution of valence states is somewhat more complicated in AES than these other techniques, it does have several distinct advantages. AES is by far the most popular technique for surface elemental analysis and is commonly found in laboratories involved in surface studies. It is simple, sensitive, relatively inexpensive, and offers a localized view of electronic properties common to the core-level techniques. From the results of several recent studies as well as our present results, it is clear that the AES technique can be an important source of information on valence-band electronic properties of solid

surfaces.

The detailed AES-SXE comparison has shown that there are striking overall similarities in the line shapes derived in the two techniques. Although the Auger selection rules and matrix-element effects are much more complex than the optic selection rules for SXE, the end effect appears to be the same. One striking difference, however, is the very small L_2 core-hole contribution to AES. This effect is predominant throughout the transition metals and is unexplained.

Although very little work has been done in exploiting core-level characteristic loss spectroscopy (CLS) as a probe of conduction-band properties, our results indicate that this technique shows great promise. The spectral shapes appear very close to those of soft-x-ray absorption while yielding the additional benefit of being surface sensitive. Also, such measurements are accomplished with identical apparatus to that used in AES.

Our comparisons of CLS and SXA structures has shown that the information derived from the two techniques is virtually identical in the threshold region. The surprising result is that the SXA data appear to contain the same structure due to low-level loss processes as do the CLS data. This suggests that the x-ray absorption process is strongly influenced by true many-body effects. This also demonstrates an advantage of CLS over SXA in that the effect of low-level losses can be removed from the CLS data while there is no such prospect for SXA. The resulting "true" structures are then more directly comparable to theoretical models as our comparisons have shown. The L_2 structure for CLS has more nearly the correct relative contribution compared to the L_3 than in the AES case.

The end purpose of the present study is not, of course, simply further evidence establishing two electron spectroscopic techniques as tools for studying surface electronic properties or the characterization of these properties for Ti and TiO_2 surfaces. Rather, it is the establishment of the relationship of such properties for Ti, TiO_2 , and other semiconductor materials to their photocatalytic behavior. Surface measurements are not, at this point, capable of probing the solid-electrolyte interface in an actual photoelectrolysis cell, but can make a definite contribution in studies of the detailed surface chemistry involved in the interaction of H_2O with the surface. By using techniques such as AES and CLS in conjunction with other surface probes such as work function measurements, electron stimulated desorption, low-energy electron diffraction, and thermal desorption spectroscopy, it is hoped that one can

establish such detailed behavior as (i) how H₂O is absorbed, (ii) how it dissociates, (iii) what are the active sites for adsorption and dissociation, and (iv) what surface chemical complexes are formed by the dissociative products.

ACKNOWLEDGMENTS

We acknowledge useful discussions with P. J. Feibelman, E. J. McGuire, and A. C. Switendick and the technical assistance of R. A. Jaramillo.

*Prepared for the U. S. ERDA under Contract No. AT(29-1)-789.

¹A. Fujishima and K. Honda, *Nature* **238**, 37 (1972).

²J. G. Mavroides, D. I. Tchernev, J. A. Kafalas, and D. F. Kolesar, *Mat. Res. Bull.* **10**, 1023 (1975).

³J. G. Mavroides, J. A. Kafalas, and D. F. Kolesar, *Appl. Phys. Lett.* **28**, 241 (1976).

⁴F. Möllers, H. J. Tolle, and R. Memming, *J. Electrochem. Soc.* **121**, 1160 (1974).

⁵V. E. Henrich, G. Dresselhaus, and J. J. Zeiger, *Phys. Rev. Lett.* **36**, 1335 (1976).

⁶C. Naccache, P. Meriaudeau, M. Che, and A. J. Tench, *Faraday Soc. Trans.* **67**, 506 (1971).

⁷F. J. Morin and T. Wolfram, *Phys. Rev. Lett.* **30**, 1214 (1973).

⁸A. H. Boonstra and C. A. H. A. Mutsaers, *J. Phys. Chem.* **79**, 1940 (1975).

⁹For a general review of the various spectroscopies, see *Physics Today* **28**, No. 4 (1975).

¹⁰C. J. Powell, *Phys. Rev. Lett.* **30**, 1179 (1973); J. E. Houston, *J. Vac. Sci. Technol.* **12**, 255 (1975).

¹¹P. J. Feibelman, E. J. McGuire, and K. C. Pandey, *Phys. Rev. Lett.* **36**, 1154 (1976); and J. E. Houston and M. G. Lagally, *J. Vac. Sci. Technol.* **13**, 361 (1976).

¹²J. S. Solomon and W. L. Baun, *Surf. Sci.* **51**, 228 (1975).

¹³D. W. Fischer, *J. Appl. Phys.* **41**, 3561 (1970).

¹⁴E. N. Sickafus, *Rev. Sci. Instrum.* **42**, 933 (1971).

¹⁵H. H. Madden and J. E. Houston, *J. Appl. Phys.* (to

be published).

¹⁶J. T. Grant, T. W. Haas, and J. E. Houston, *J. Vac. Sci. Technol.* **11**, 227 (1974); P. J. Bassett and T. E. Gallan, *J. Electron Spectrosc. Relat. Phenom.* **2**, 101 (1973).

¹⁷R. L. Gerlach and D. W. Tipping, *Rev. Sci. Instrum.* **42**, 151 (1971).

¹⁸J. E. Houston and R. L. Park, *Rev. Sci. Instrum.* **43**, 1437 (1972).

¹⁹R. L. Gerlach, J. E. Houston, and R. L. Park, *Appl. Phys. Lett.* **16**, 179 (1970).

²⁰P. H. Van Cittert, *Z. Phys.* **69**, 304 (1931).

²¹D. W. Fischer and W. L. Baun, *J. Appl. Phys.* **39**, 4757 (1968).

²²J. E. Houston and R. L. Park, *J. Chem. Phys.* **155**, 4601 (1971); and C. Nyberg, *Surf. Sci.* **52**, 1 (1972).

²³O. Jepsen, *Phys. Rev. B* **12**, 2988 (1975).

²⁴D. W. Fischer, *J. Appl. Phys.* **41**, 3922 (1970).

²⁵P. J. Feibelman, E. J. McGuire, and K. C. Pandey, *Phys. Rev. B* **15**, 2202 (1977).

²⁶P. W. Palmberg, G. E. Rlach, R. E. Weber, and N. C. MacDonald, *Handbook of Auger Electron Spectroscopy* (Physical Electronics Industries, Edina, Minn., 1972).

²⁷R. Ludeke and A. Koma, *Phys. Rev. Lett.* **34**, 817 (1975).

²⁸J. L. Freeouf, *Phys. Rev. Lett.* **36**, 1095 (1976).

²⁹O. Keski-Rahkonen and M. O. Krause, *At. Data Nucl. Data Tables* **14**, 139 (1974).